Original Article

Evaluation of MCNPX and GATE with HotSpot for Internal Dosimetry (Simulation Study)

Hadi Taleshi Ahangari[1*], Ali Ghanbari[2], Nasroallah Moradi kor[2]

[1]*Department of Medical Physics, Faculty of Medicine, Semnan University of Medical Sciences, Semnan, Iran*
[2]*Physiology Research Center, Faculty of Medicine, Semnan University of Medical Sciences, Semnan, Iran*

A R T I C L E   I N F O

A B S T R A C T

Objective: Different categories are available for estimating of radiation dose. Radioisotopes with the same energy and almost the same physical properties have similar effects. Monte Carlo technique is a computerized method based on mathematical simulation of physical processes. The main purpose of this study is to show that beta particles are not able to penetrate deep into the water. also difference between GATE and MCNP code is not significant. **Methods:** In this study, a digital form of the cylinder mathematical phantom was constructed and used with GATE and MCNPX to calculate the phantom dose. The voxel-based anthropomorphic Zubal phantom was used to model a typical adult male. The equivalent effective dose derived for the electrons of Er-169, P-32, and Y-90 with GATE and MCNPX. The results were compared to the HOTSPOT data. **Results:** The GATE and MCNPX difference was negligible. However, difference at this level is acceptable and we can conclude that GATE produces almost similar results as MCNPX. In this study, we tried to set the physical framework, calculate the penetration depth via dosimetry, using the results of the two simulator codes. In the first part, we applied the results of the HotSpot dosimetry software for validation. **Conclusion:** The GATE and MCNPX difference was negligible.

1. INTRODUCTION

Different categories are available for estimating and assessment of radiation dose and biological effects in therapeutic and diagnostic nuclear medicine (McGoron, 2002; Hamoudeh et al., 2008; Qaim, 2001; Sartor et al., 2013;Das and Pillai, 2013; Pouget et al., 2015). These categories are on the basis of: 1) importance of biological effects, 2) energy, 3) radionuclide half-life, 4) state of matter (gas or solid), 5) importance of imaging procedure, 6) therapeutic importance,7) cross-section of the collisions. Radioisotope categorization is also important because radioisotopes with the same energy and almost the same physical properties have similar biological effects on the human body (Bardies and Chatal, 1994;Jakson et al., 2013). Er-169 decays under emission of beta particles to stable thulium. The maximum energy of the beta particles is 0.34 MeV. Average penetration depth in the tissue is 0.3 mm and the half-life is equal to 9.4 days (http://atom.kaeri.re.kr/ton/). This radio pharmaceutical can be used in pain reduction treatments in small joints in the form of citrate complex. The injected dose is approximately 0.5 and 1 mCi and the maximum injection would be 20 mCi (Eary and Brenner, 2007).

Corresponding Author: Hadi Taleshi Ahangari, Department of Medical Physics, Faculty of Medicine, Semnan University of Medical Sciences, Semnan, Iran (Taleshi@semums.ac.ir)

Phosphorus-32 is a beta emitter with a half-life of 14.3 days and average energy of 0.693 Kev (http://atom.kaeri.re.kr/ton/). Because of the nature of iniquitousness, it is used in the treatment of systemic cancers. However, participants' treatment with Phosphorus-32 can cause blood poisoning (Mathew et al., 2000). Also Bremsstrahlung imaging was accomplished with phosphorus -32 (Balachandran et al., 1985).

Y-90 with a maximum of 2.3 MeV is a beta emitter and a good choice for treatment (http://atom.kaeri.re.kr/ton/).

It is suitable for the treatment of larger tumors due to higher energy and penetration depth in the tissue. This radionuclide has the maximum penetration depth of 1.2 cm in water (Eary and Brenner, 2007; Ito et al., 2009). The most accurate way of calculating electrons and photon interactions with matter has been the Monte Carlo method (Mainegra-Hing et al., 2005), as a result of which the absorption dose distribution in matter can be achieved.

Table 1:

Summary of decay data for three major beta emitter radionuclides

Radionuclide	Half-life(d)	Max. beta energy (MeV)	Ave. beta energy (Kev)	Max. range (mm)	Mean range (mm)
Erbium-169	9.4	0.34	~100	1.0	0.3
Phosphorus-32	14.3	1.71	695	7.9	2.6 (¬ 1.85)
Yttrium-90	2.7	2.27	934	11	3.6 (¬2.76)

Monte Carlo codes are much faster and more flexible for simulating beam interactions and dose measurements in human phantoms than the practical methods. Monte Carlo technique is a computerized and calculational method based on mathematical simulation of physical processes. To implement these techniques in a computer, physical processes should be based on the rules governing the probability formulation. In this way, the history of beam interactions with a large number of collisions are traced with the use of physical description of interactions and the amount of energy released and absorbed per interaction. Computational Monte Carlo method is time consuming, and the methods based on the application of the Monte Carlo will be more useable in case of progression in the speed of computer systems (Zaidi and Erwin, 2007). Using codes that can be able to simulate the beam transportation can be a remarkable improvement in the accuracy of dose calculations. Today, the majority of dose absorption calculations in nuclear medicine are in the form of theoretical calculations with low accuracy. Limitations of analytical methods and low accuracy have led to the application of the Monte Carlo technique in determining the dose absorption, and with extended progresses in computer systems, Monte Carlo methods can be used in modelling the transfers of hazardous and physical models. Monte Carlo calculation methods are efficient in practice where dosimetry may not be very costly (Rodrigues et al., 2004; Sqouros and Hobbs, 2014).

GATE which is based on the GEANT 4 package is the most recently developed Monte Carlo code with the ambition of becoming the gold standard code in nuclear medicine. GATE is practically the only nuclear medicine dedicated code with options for different types of imaging and determining the dose distribution inside the body. It includes a very flexible simulation geometry input capable to accommodate a large variety of detector and source geometries. It also includes a user-friendly implemented voxelized source and a virtual clock to allow simulation of temporal phenomena such as source and detector movements and source decay. GATE is very flexible for simulating complex detector geometries and experimental arrangements. Although GATE is an almost validated code (Parach et al., 2011; Maigne et al., 2011; Parach and Rajabi, 2010; Jan et al., 2011; Assie et al., 2005) but it is itself a new code and less experienced compared to older codes like MCNP, and not properly validated. Moreover, the results of this code have never been compared against older Monte Carlo packages like MCNP. General-purpose codes like MCNP and EGS have extensively been validated for different applications. Making comparisons with these codes may be considered as an essential step in validation of new codes like GATE (Parach and Rajabi, 2010). The HotSpot Health Physics Code which is used for safety-analysis of department of energy, facilities nuclear material handling. HotSpot incorporates Federal Guidance Reports 11, 12, and 13 (FGR-11, FGR-12, FGR-13) and Dose Conversion Factors (DCFs) for inhalation, submersion, and ground shine (Homann, 2011).

In this study, the digital form of the cylinder mathematical phantom was constructed and used with GATE and MCNPX to calculate the dose of the phantom. The results were compared to the HOTSPOT data. The purpose of this study is to show that beta particles are not able to penetrate deep into the water, and also it has further recommendations for clinical applications.

2. MATERIALS AND METHODS

2.1. Stopping power
Distance is very efficient for radiation protection as the dose falls off in square; hence, at far physical distances the total dose is negligible. However, the simulation time and errors can be decreased significantly by phantom volume.

The electron stopping power represents the mean energy loss per unit path length ,and it is defined as (Berger, 1988).

Stopping power = -dE/dx

When the path length increment (dx) is expressed in mass units, the stopping power is called the mass stopping power.

$S = (dE/dX)/\rho$, $[S] = MeV/(g/cm^2)$

ESTAR calculates the stopping-power and range tables for electrons according to methods described in ICRU reports [37, 49]. The codes provide output for electrons in any stopping material.

The energy loss per unit path length fluctuates strongly about the average values given by the stopping powers. The use of the continuous-slowing-down approximation (CSDA) simplifies and speeds up dose calculations. Effective range for three radioisotopes in air is given in the following table.

Table 2:
Effective radius dose of three major beta emitter radioisotopes in the air

Radioisotope	$Distance(m)$
Er-169	**1**
P-32	**7.5**
Y-90	**10**

2.2. Software
Hotspot software (version 2.07.2) has extensively been validated for different applications. Comparison to this software may be considered as an essential step in validation of new dosimetery calculations.

2.3. Simulation System
For the simulation of the computer core i -7 2630QM was used by making the MPICH 2 software to cluster CPU in parallel. GATE Monte Carlo package (version 6.1) and MCNPX (version 2.6.02) were used for estimation of equivalent effective dose to the phantoms. X-rays were tracked down to 1 Key, below which was assumed as absorbed in the same voxel. Ionization, multiple scattering, and bremsstrahlung were considered for electron interactions. The cut off range applied on the secondary electrons was 1 mm. Each voxel in the phantoms was linked to the table describing the attenuation properties (composition and density) of the corresponding water [Parach and Rajabi, 2010]. Simulations were performed for three radioisotopes, Er-169, P-32, and Y-90. For the electrons 5.0 × 107, histories were tracked, and the dose deposited in each voxel of the phantoms in cGy was determined.

2.4. Phantoms
The sphere phantom and the Zubal phantom were used in this study. The sphere phantom (radius 15cm) consisted of 64 × 64 × 64 voxels of 4 × 4 × 4 mm dimensions. In order to define a standard phantom, equivalent with ICRU sphere phantom, water was used (Thomas, 2012).

Fig. 1: ICRU Sphere phantom (radius 15 cm) and a radioactive source (internal radius 15 cm and external radius 25 cm).

The voxel-based anthropomorphic Zubal phantom was used to model a typical adult male (Zubal et al., 1994). The phantom included head and body torso (no arms or legs) segmented into 56 different tissue types. The phantom consisted of 128 × 128 × 243 voxels of 4 × 4 × 4 mm dimensions. It was generated and the activity was distributed uniformly within the liver of the phantoms. This geometry was exactly the same as the geometry used by (Yoriyaz et al., 2000; Chiavassa et al., 2006; Parach and Rajabi, 2010).
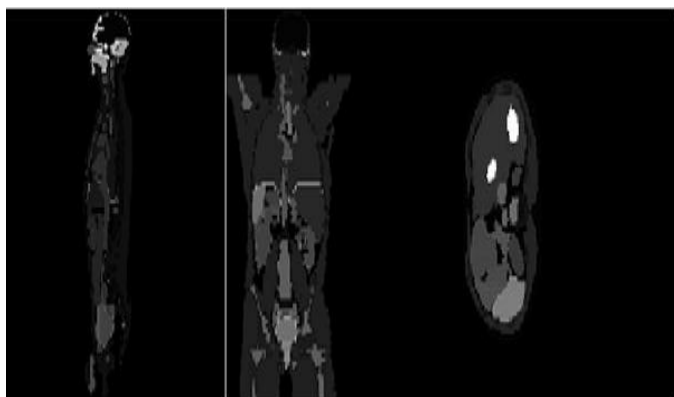
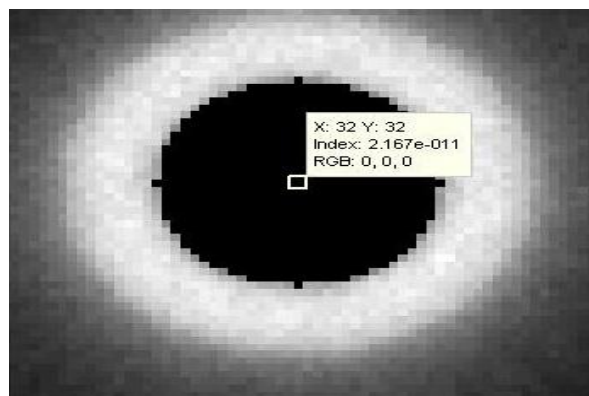**Fig. 2:** Zubal phantom in coronal, sagittal and transverse

Fig. 3: Y-90 radionuclide distribution (external radius 25 cm).

3. RESULTS

The equivalent effective dose derived for the electrons of Er-169, P-32, and Y-90 using Hotspot Software are represented in Tables 3, 4, and 5.

Table 3:
Equivalent effective dose of Er -169 in the Hotspot software

Er-169							
	Air submersion dose conversion factors ([sievert-m3]/[Becquerel-sec])						
	R Marrow	1.22E-18	ULI Wall	1.03E-18	Adrenals	1.03E-18
	Lung	1.49E-18	LLI Wall	9.42E-19	Skin	2.80E-15
	Sl Wall	9.32E-19	Kidneys	1.36E-18	Spleen	1.24E-18
	Thyroid	1.79E-18	Liver	1.26E-18	Testes	1.96E-18
	Breast	2.46E-18	Bld Wall	1.16E-18	Thymus	1.46E-18
	Esophagus	8.72E-19	Muscle	1.66E-18	Brain	1.38E-18
	St Wall	1.24E-18	Ovaries	8.54E-19	Uterus	8.89E-19
	B Surface	5.84E-18	Pancreas	8.82E-19		
					EDE	1.74E-18

Table 4:
Equivalent effective dose of P-32 in the Hotspot software

P-32	Air submersion dose conversion factors ([sievert-m3]/[Becquerel-sec])					
	R Marrow	8.20E-17	ULI Wall	7.07E-17	Adrenals	7.09E-17
	Lung	9.09E-17	LLI Wall	6.76E-17	Skin	4.49E-14
	Sl Wall	6.66E-17	Kidneys	8.11E-17	Spleen	8.00E-17
	Thyroid	9.74E-17	Liver	8.00E-17	Testes	9.90E-17
	Breast	1.16E-16	Bld Wall	7.41E-17	Thymus	8.61E-17
	Esophagus	6.70E-17	Muscle	9.13E-17	Brain	9.20E-17
	St Wall	7.87E-17	Ovaries	6.37E-17	Uterus	6.48E-17
	B Surface	2.48E-16	Pancreas	6.56E-17		
					EDE	9.90E-17

Table 5:
Equivalent effective dose of Y-90 in the Hotspot software

Y-90	Air submersion dose conversion factors ([sievert-m3]/[Becquerel-sec])					
	R Marrow	1.62E-16	ULI Wall	1.39E-16	Adrenals	1.40E-16
	Lung	1.77E-16	LLI Wall	1.34E-16	Skin	6.23E-14
	Sl Wall	1.32E-16	Kidneys	1.57E-16	Spleen	1.56E-16
	Thyroid	1.87E-16	Liver	1.56E-16	Testes	1.89E-16
	Breast	2.20E-16	Bld Wall	1.44E-16	Thymus	1.67E-16
	Esophagus	1.34E-16	Muscle	1.76E-16	Brain	1.81E-16
	St Wall	1.54E-16	Ovaries	1.27E-16	Uterus	1.29E-16
	B Surface	4.43E-16	Pancreas	1.30E-16		
					EDE	1.90E-16

The equivalent effective dose (sphere phantom) is derived using MCNPX, and Gate is also included in the Tables for the sake of comparison. The data in each Table are analyzed independently, and the results are presented.

Table 6:
Equivalent effective dose of Er -169 in MCNPX

Source radius (cm)	1	2	5	10	20	50	100
f6 Tally electron	5.96E-09	6.55E-09	7.24E-09	7.55E-09	7.64E-09	7.64E-09	7.64E-09
f6 Tally photon	5.92E-09	6.49E-09	7.19E-09	7.49E-09	7.59E-09	7.59E-09	7.59E-09
Dose ([Gy-m3]/[Bq-sec])	9.54E-19	1.05E-18	1.16E-18	1.21E-18	1.22E-18	1.22E-18	1.22E-18

Table 7:
Equivalent effective dose of P-32 in MCNPX

Source radius (cm)	1	2	5	10	20	50	100
f6 Tally electron	8.76E-08	8.97E-08	9.27E-08	9.42E-08	9.48E-08	9.48E-08	9.48E-08
f6 Tally photon	2.73E-08	2.93E-08	3.23E-08	3.38E-08	3.44E-08	3.44E-08	3.44E-08
Dose([Gy-m3]/[Bq-sec])	1.84E-17	1.90E-17	2.00E-17	2.05E-17	2.07E-17	2.07E-17	2.07E-17

Table 8:
Equivalent effective dose of Y-90 in MCNPX

Source radius (cm)	1	2	5	10	20	50	100
f6 Tally electron	9.61E-07	9.65E-07	9.70E-07	9.73E-07	9.74E-07	9.74E-07	9.74E-07
f6 Tally photon	5.01E-08	5.40E-08	5.92E-08	6.19E-08	6.29E-08	6.30E-08	6.30E-08
Dose ([Gy-m3]/[Bq-sec])	1.62E-16	1.63E-16	1.65E-16	1.66E-16	1.66E-16	1.66E-16	1.66E-16

Table 9:

Equivalent effective dose for three radioisotope in GATE *(Gy/Bq.Sec)*

Source radius (cm)	1	2	5	10	15	20
Er-169	5.12E -18	3.09E -19	1.33E -19	4.52E -20	2.39E -20	1.69E -20
P-32	6.01E -18	2.82E -18	8.18E -19	3.94E -19	2.46E -19	1.76E -19
Y-90	9.69E -18	3.53E -18	1.07E -18	4.92E -19	3.07E -19	2.10E -19

Table 10:

Calculation of equivalent effective dose in the Zubal phantom

|	Y-90 (cGy/Bq.sec)	P-32 (cGy/Bq.sec)	Er-169 (cGy/Bq.sec)
Adipose	1.26576E-15	5.8775E-16	0
Air	1.58968E-15	6.16431E-16	0
Blood	4.69566E-13	2.61669E-13	2.61669E-13
Body	2.19969E-12	1.35675E-12	5.30246E-14
Brain	2.78745E-13	1.5678E-13	7.25265E-15
Cartilage	6.82361E-14	3.91435E-14	1.37485E-15
Heart	2.77754E-13	1.72685E-13	7.77254E-15
Intestin	3.57383E-13	2.24691E-13	9.23579E-15
Kidney	1.42509E-13	8.78024E-14	3.67517E-15
liver	1.14904E-12	7.4853E-13	3.11639E-14
Lung	2.0098E-12	1.50577E-12	1.29817E-13
Muscle	4.0389E-12	2.46642E-12	1.00176E-13
Pancreas	1.60689E-14	7.29313E-15	1.49693E-16
Rib bone	1.73135E-12	1.1938E-12	1E-13
Skull	5.52756E-14	2.78908E-14	1.10539E-15
Spine bone	1.13542E-16	3.43552E-17	0
Spleen	7.31916E-14	4.08725E-14	1.81278E-15
Water	5.70903E-13	3.43491E-13	1.29946E-14
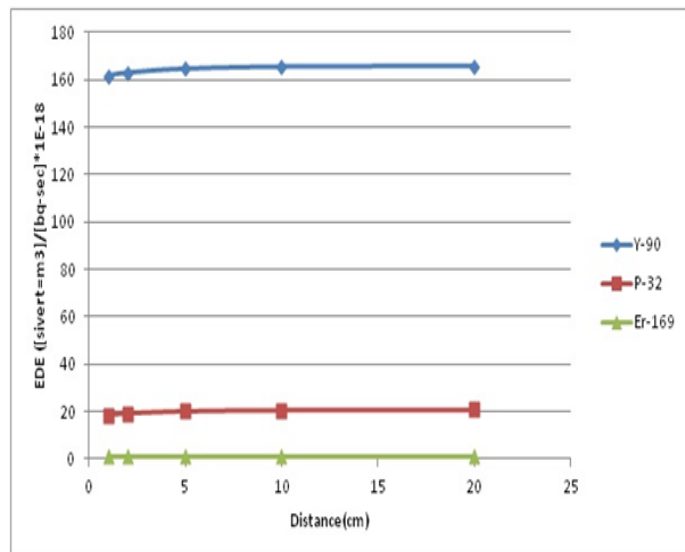
Fig. 4: Radioisotopes dose rate in various distances
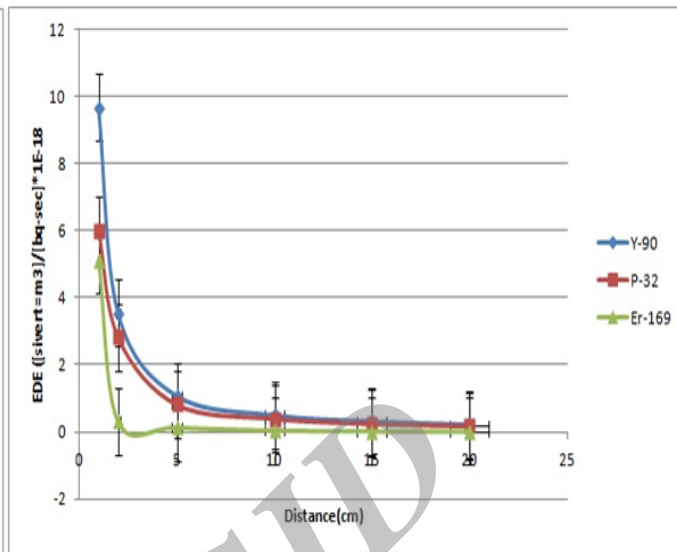

Fig. 5: Radioisotopes absorbed dose in various distances

4. DISCUSSION

The aim of the present study was to compare Gate and MCNPX with the older and well-developed Monte Carlo code constituting a validation of Gate and MCNPX for health physics dosimetry. The Hotspot software was used for this comparison. It was assumed the activity in the whole of liver, kidneys and thyroid has distributed uniformly and using EGS4 and MCNPx 2.5e codes determined absorbed dose to the organs from internal radiations of ^{131}I in voxel phantoms, Zubal, and compared them (Chiavassa et al. 2006). Obtained S-values, using two approaches, were good agreed together with a difference lower than 10%. Of course, the results were agreed in photons more than electrons. So that in MCNPX, absorbed dose calculated for electrons in some tissues was zero and in EGS4, was shown a small amounts of absorbed dose. In our study, Comparison of GATE and MCNPX showed well that difference will be lower than 5%. In 2007, to validate of GATE code, Ferrer and colleagues compared absorbed doses of 10 KeV electrons in simulation codes, MCNPX and GATE. Also, absorbed dose calculated using GATE was compared with other published values. They showed that the absorbed dose obtained by using GATE and MCNPX codes was agreed together well, Thus can be said to GATE code can be used for simulating and determining absorbed dose in nuclear medicine in humans or animals (Ferrer et al. 2007). The results are in good agreement with our research. Furthermore, in several studies, beta particles'

penetration in air and water is calculated, and the results are reported. However, as it was mentioned, how far source to target organs. In this study, we tried to set the physical framework, calculate the penetration depth via dosimetry, using the results of the two simulator codes. In the first part, we applied the results of the HotSpot dosimetry software for validation. Since the beta particles' penetration depth is statistically significant, and generally the average penetration depth is considered, the purpose was to examine this issue. In physics, the maximum beta particles' penetration and the average penetration depth of radioisotopes depend on energy. However, the simulation, results showed that there were slight changes in different intervals which could be estimated. Bardies et al. 2006) expressed that absorbed dose each voxel can be calculated by activity determination at the same voxel, and Monte Carlo calculations can be used for calculating absorbed dose. Also, they expressed that Monte Carlo calculations can be standardized and formulated and used in practical and clinical applications. Nevertheless, our research showed the activity can affect on the other voxels. The absorbed dose was investigated by voxels, and it was proved that it could be a good approximation with an average radius. The results are presented in Figure 5. In Zubal phantom, as expected, the influence of beta particles' penetration was found. Hence, the equivalent effective dose couldn't be calculated with the radioisotope penetration depth.

CONCLUSION

The GATE and MCNPX difference was negligible. However, difference at this level is acceptable and we can conclude that GATE produces almost similar results as MCNPX. In general, the agreement is acceptable and the results can be considered as validation of GATE and MCNPX against HotSpot Software; however, some issues require further investigation.

Conflict of interest statement

We declare that we have no conflict of interest.

REFERENCES

Assié, K., Gardin, I., Vera, P., Buvat, I. (2005). Validation of the monte carlo simulator GATE for indium-111 imaging. *Phys Med Biol*, 50(13): 3113-3125.

Balachandran. S., McGuire, L., Flanigan, S., Shah, H., Boyd, C.M. (1985). Bremsstrahlung imaging after 32P treatment for residual suprasellar cyst. *Int J of Nuc Med and Biol,* 12(3): 215- 221.

Bardies, M., Chatal, J.F. (1999). Absorbed doses for internal radiotherapy from 22 beta-emitting radionuclides: beta dosimetry of small spheres. *Phys Med Biol,* 39(6): 961.

Berger, M.J. (1988). Electron stopping powers for transport calculations. Monte Carlo Transport of Electrons and Photons, Springer**:** 57-80.

Chiavassa, S., Aubineau-Laniece, I., Bitar, A., Lisbona, A., Barbet, J., Franck, D., et al. (2006). Validation of a personalized dosimetric evaluation tool (Oedipe) for targeted radiotherapy based on the monte carlo MCNPX code. *Phys Med Biol,* 51(3): 601-616.

Das, T., & Pillai, M. R. A. (2013). Options to meet the future global demand of radionuclides for radionuclide therapy. *Nucl Med Biol*, 40(1), 23-32.

Eary, J.F., Brenner, W. (2007). Nuclear medicine therapy. Taylor and Francis, New York, London, ISBN-13: 9780824728762, Pages: 216.

Hamoudeh, M., Kamleh, M.A., Diab, R., Fessi, H. (2008). Radionuclides delivery systems for nuclear imaging and radiotherapy of cancer. *Adv Drug Deliv Rev,* 60:1329-46.

Ito, S., Kurosawa, H., Kasahara, H., Teraoka, S., Ariga, E., Deji, S. (2009). ^{90}Y bremsstrahlung emission computed tomography using gamma cameras. *Ann Nucl Med,* 23(3): 257-267.

Jackson, M. R., Falzone, N., & Vallis, K. A. (2013). Advances in anticancer radiopharmaceuticals. *Clin Oncol*, *25*(10), 604-609.

Jan, S., Benoit, D., Becheva, E., Carlier, T., Cassol, F., Descourt, P., et al. (2011). GATE V6: a major enhancement of the GATE simulation platform enabling modelling of CT and radiotherapy. *Phys Med Biol,* 56(4): 881.

Maigne, L., Perrot, Y., Schaart, D.R., Donnarieix, D., Breton, V. (2011). Comparison of GATE/GEANT4 with EGSnrc and MCNP for electron dose calculations at energies between 15 keV and 20 MeV. *Phys Med Biol,* 56:811.

Mainegra-Hing, E., Rogers, D., Kawrakow, I. (2005). Calculation of photon energy deposition kernels and electron dose point kernels in water. *Medical Physics,* 32: 685.

Mathew, P., Talbut, D., Frogameni, A., Singer, D., Chrissos, M., Khuder, S., et al. (2000). Isotopic synovectomy with P-32 in paediatric patients with haemophilia. 6:547-55.

McGoron, A. J. (2002). Radioisotopes in Nuclear Medicine. Proceedings of the Americas Nuclear Energy Symposium, October 16-18, 2002, U.S. Department of Energy, Miami, Florida International University.

Parach, A., Rajabi, H. (2011). A comparison between GATE4 results and MCNP4B published data for internal radiation dosimetry. *Nuklearmedizin-Nuclear Medicine,* 50(3): 122.

Parach, A.A., Rajabi, H., Askari, M.A. (2011). Assessment of MIRD data for internal dosimetry using the GATE Monte Carlo code. *Rad environ biophys,* 50(3): 441-450.

Pouget, J. P., Lozza, C., Deshayes, E., Boudousq, V., & Navarro-Teulon, I. (2015). Introduction to radiobiology of targeted radionuclide therapy. *Front Med*, *2*.

Qaim, S.M. (2001). Therapeutic radionuclides and nuclear data. Radiochimica Acta. *Int J Chem Aspects Nucl Sc Technol,* 89:297.

Rodrigues, P., Trindade, A., Peralta, L., Alves, C., Chaves, A., Lopes, M.C. (2004). Application of GEANT4 radiation transport toolkit to dose calculations in anthropomorphic phantoms. *Appl Radiat Isotopes,* 61(6): 1451-1461.

Sartor, O., Hoskin, P., & Bruland, Ø. S. (2013). Targeted radio-nuclide therapy of skeletal metastases. *Cancer treatment reviews*, *39*(1), 18-26.

Sgouros, G., & Hobbs, R. F. (2014, May). Dosimetry for radiopharmaceutical therapy. In *Semin Nucl Med* (Vol. 44, No. 3, pp. 172-178). WB Saunders.

Thomas, D.J. (2012). ICRU report 85: fundamental quantities and units for ionizing radiation. *Radiation Protection Dosimetry,* 150(4): 550-552.

Volkert, W.A., Goeckeler, W.F., Ehrhardt, G.J., Ketring, A.R. (1991). Therapeutic Radionuclides:Production and Decay Property Considerations. *J Nucl Med,*32(1): 174-8.

Yoriyaz, H., et al. (2000). Absorbed fractions in a voxel-based phantom calculated with the [small-caps MCNP-4B] code. *Med Phys,* 27: 1555.

Zaidi, H. Erwin, W.D. (2007). Quantitative Analysis in Nuclear Medicine Imaging. *J Nucl Med,* 48(8): 1401.

Zubal, I.G,, Harrell, C.R., Smith, E.O., Rattner, Z., Gindi, G., Hoffer, P.B. (1994). Computerized three-dimensional segmented human anatomy. *Med Phys,* 21(2) :299.